Journal of Crystal Growth 311 (2009) 2109–2112

Contents lists available at ScienceDirect

Journal of Crystal Growth

journal homepage: www.elsevier.com/locate/jcrysgro

Wide band gap II–VI selenides for short wavelength intersubband devices

A. Shen [a,*], W.O. Charles [a], B.S. Li [a,b], K.J. Franz [c], C. Gmachl [c], Q. Zhang [d], M.C. Tamargo [e]

[a] Department of Electrical Engineering, The City College of the City University of New York, NY 10031, USA
[b] School of Physics and Engineering, Sun Yat-Sen University, Guangzhou 510225, China
[c] Department of Electrical Engineering, Princeton University, Princeton, NJ 08544, USA
[d] Department of Physics, The City College of the City University of New York, NY 10031, USA
[e] Department of Chemistry, The City College of the City University of New York, NY 10031, USA

ARTICLE INFO

Available online 8 November 2008

PACS:
81.05.Dz
81.07.St
81.15.Hi
85.35.Be

Keywords:
A3. Molecular beam epitaxy
B1. MgSe
B1. ZnCdSe
B1. ZnCdMgSe
B2. Semiconducting II–VI materials
B3. Infrared devices

ABSTRACT

In this paper, we present our recent progress towards the realization of short wavelength intersubband devices with wide band gap II–VI selenide semiconductors. Intersubband electroluminescence at 4.8 μm was observed in a ZnCdSe/ZnCdMgSe quantum cascade structure at temperatures up to room temperature. We also developed a new ZnCdSe/MgSe quantum structure with metastable MgSe barriers. Intersubband absorption in the 3–5 μm range was observed. Calculations suggest that with this structure intersubband transitions as short as 1.55 μm may be achieved.

© 2008 Elsevier B.V. All rights reserved.

1. Introduction

Advanced quantum devices based on intersubband (ISB) transitions in semiconductor low-dimensional structures have been extensively studied during the past two decades. These devices, developed through the convergence of band structure engineering [1] and molecular beam epitaxy (MBE) [2], range from emitters–quantum cascade (QC) lasers [3], to detectors–quantum well (QW) infrared (IR) photodetectors [4], and all-optical switches and modulators [5]. One of the major advantages of ISB devices is the ability to tune the operating wavelength independently of the material band gap. For example, high-performance QC lasers realized with InGaAs/InAlAs QWs can cover the spectral range from 4 to 24 μm [6]. Recently, significant efforts have been made to extend the wavelength range of the QC lasers. On the long wavelength side, to reach the terahertz (30–300 μm) range, completely new design strategies must be adopted, such as using electron–electron scattering to replace the electron–phonon scattering [7] or spatially separating the phonon scattering region from the optical transition region [8]. On the short wavelength side, however, new material systems must be explored, since the shortest wavelength achievable is determined by the available conduction band offset (CBO), ΔE_c, in a material system.

One material system that has been extensively studied for short wavelength ISB devices is the antimonide-based heterostructures, including InGaAs/AlAsSb on InP substrates and InAs/AlSb on InAs substrates. Although at present the performance of Sb-based QC devices is not comparable to that of InGaAs/InAlAs QC lasers operating in the 5–12 μm spectral range, very impressive results have been reported [9,10]. In addition to Sb-based heterostructures, nitride-based materials have also been investigated for short wavelength ISB devices. Recently, ISB photoluminescence at 2.13 μm in GaN/AlN QWs has been reported [11].

We have proposed the use of wide band gap II–VI semiconductors as an alternative material system for short wavelength ISB devices [12]. In this paper, we summarize our results of ISB electroluminescence (EL) in ZnCdSe/ZnCdMgSe QC structures. Furthermore, a new ZnCdSe/MgSe QW structure with metastable MgSe barriers was grown and characterized. Calculations indicate that ISB transition at wavelengths as short as 1.55 μm can be achieved in ZnCdSe/MgSe coupled QWs, making the material a promising candidate for ultrafast all-optical switches operating at optical communication wavelengths.

2. ZnCdSe/ZnCdMgSe QC structure

A ZnCdSe/ZnCdMgSe QC structure has been designed and growth by MBE [13]. A single stage of the layer sequence in angstroms, starting from the injection barrier, is: ***30***/*34*/***10***/*28*/***20***/

*Corresponding author.
E-mail addresses: aidong_s@yahoo.com, aidong@sci.ccny.cuny.edu (A. Shen).

0022-0248/$ - see front matter © 2008 Elsevier B.V. All rights reserved.
doi:10.1016/j.jcrysgro.2008.10.102

24/**10**/22/**12**/20/**16**/20/**18**/18/**18**/18/**20**/16/**20**/16/**20**/14/**22**/14/**24**/12/**26**/12. $Zn_{0.20}Cd_{0.19}Mg_{0.61}Se$ barriers are in boldface and $Zn_{0.43}Cd_{0.57}Se$ wells are in normal font. The active region (shown in italic font) is a conventional asymmetric coupled QW structure consisting of two wells of 34 and 28 Å in thickness separated by a 10-Å-thick barrier. The asymmetric coupled QWs produce a three-level vertical transition system, with the designed emission comes from the transition between levels 3 and 2. The energy separation between levels 2 and 1 (ground level) is designed to be in resonance with the longitudinal optical (LO) phonon energy of ZnCdSe so that electrons at level 2 can be quickly depopulated by LO phonon scattering. Under the normal operating voltage, the miniband in the injector is aligned so that electrons depopulated to level 1 is injected into the level 3 of the next stage by resonant tunneling. The center region of the injector (underlined layers) is doped with Cl to $2\times10^{17}\,cm^{-3}$ using $ZnCl_2$ as dopant material. The doping in the injector region provides an electron reservoir so that the injector is not depleted at threshold. The structure is designed to emit at 4.5 μm under an applied field of $67\,kV\,cm^{-1}$. Ten periods of the active region-injector layer sequence were grown on a low-doped ($<2\times10^{17}\,cm^{-3}$) InP:S substrate. The epilayers were fabricated into 400-μm-diameter circular mesas. EL spectra were collected from the cleaved facets at various temperatures and under different injection current densities.

Fig. 1 shows the EL spectra under two different injection current densities at heat sink temperatures from 78 to 300 K. At low temperatures (<130 K) and under low injection current, a single emission peak centered at 4.8 μm was observed, which agrees well with our designed value. At higher temperatures or under higher injection current densities, a second peak at longer wavelength begins to appear. The origin of that second peak is still under investigation. Polarization-dependent measurements showed that the two peaks are TM-polarized, indicating that they both originate from ISB transitions.

The voltage–current (V–I) and light–current (L–I) characteristics of the QC structure are shown in Fig. 2. The V–I characteristics are typical for transport through QC structures. At low voltages, the resistance of the sample is high owing to level misalignment. At a voltage of about 5 V, corresponding to an electric field of $90\,kV\,cm^{-1}$, the energy levels align and the resistance drops. The turn-on field required is somewhat higher than the designed value of $67\,kV\,cm^{-1}$, possibly due to the non-ideal top contacts. At low temperatures, the L–I characteristics are almost linear. The superlinear L–I behaviour at high temperatures are most likely due to the onset of the second emission peak.

3. ZnCdSe/MgSe QWs with metastable MgSe barriers

To fully utilize the maximum CBO in this II–VI selenide material system, ZnCdSe/MgSe QWs have been proposed and grown by MBE [14]. MgSe is nearly lattice-matched to InP (with ~0.2% mismatch). With slight strain compensation from ZnCdSe, ZnCdSe/MgSe QWs can be grown lattice-matched on InP substrates. The large CBO of 1.2 eV in the structure make it possible to achieve ISB transitions in the near-IR region. MgSe, however, favours the rocksalt structure. Thus, to maintain the metastable zincblende MgSe in the QW structure, the insertion of thick ZnCdSe spacer layers was needed.

A set of three samples with 30 ZnCdSe QWs but different well thickness of 3.2, 3.8 and 4.4 nm, respectively, were grown by MBE. The MgSe barrier thickness is 5.9 nm in all the samples. A 30-nm-thick ZnCdSe spacer layer was inserted between every 2 QWs (each 2-QW unit consists of the following layer sequence: MgSe/ZnCdSe/ MgSe/ZnCdSe/MgSe). A schematic diagram of the layered structure of the samples is shown in Fig. 3. The well region is

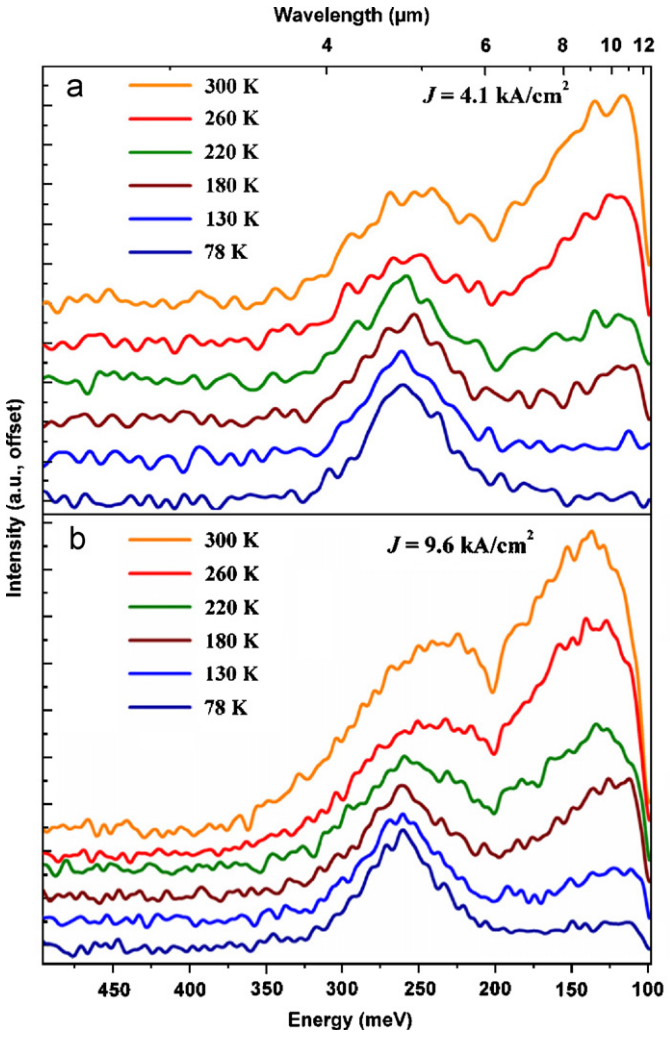

Fig. 1. EL spectra of a ZnCdSe/ZnCdMgSe QC structure collected at heat sink temperatures from 78 to 300 K under injection current density of (a) $4.1\,kA\,cm^{-2}$ and (b) $9.6\,kA\,cm^{-2}$.

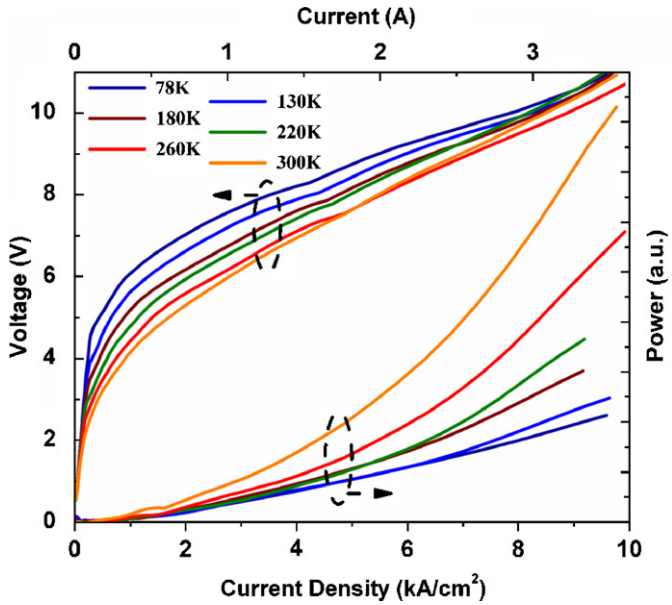

Fig. 2. Voltage-current and light-current characteristics of the QC device at temperatures from 78 to 300 K.

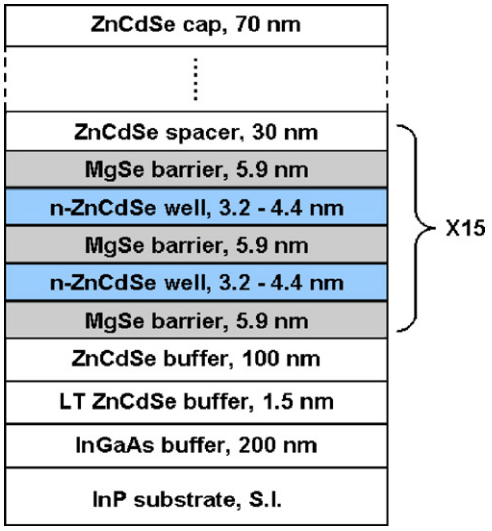

Fig. 3. A schematic drawing of the ZnCdSe/MgSe MQW structure.

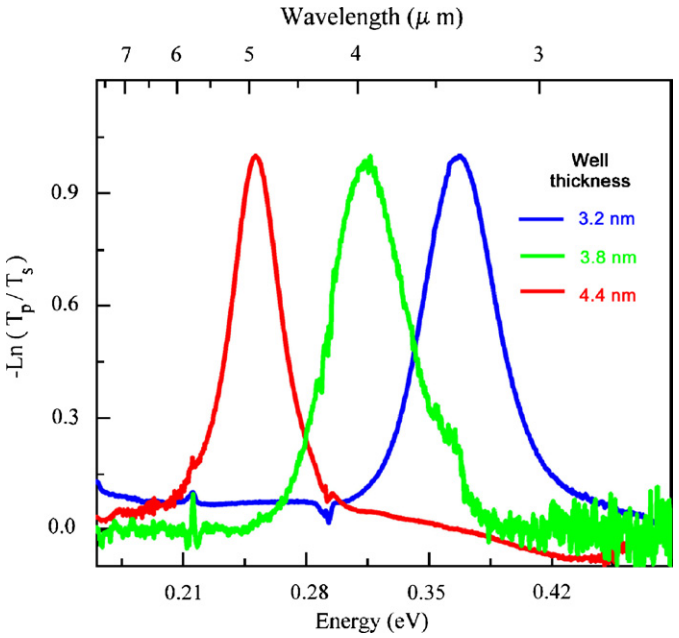

Fig. 4. ISB absorption spectra of a set of ZnCdSe/MgSe QWs at room temperature.

uniformly doped with Cl to $(1–2)\times10^{18}\,cm^{-3}$. The samples were polished into multi-pass waveguide geometry with parallel 45° facets for ISB absorption measurements. Fig. 4 shows the normalized absorbance of the three samples obtained by room-temperature Fourier transform IR spectroscopy measurements. ISB absorption in the 3–5 μm mid-IR region was observed.

Calculations based on the envelope function approximation indicate that the shortest ISB transition wavelength achievable with the ZnCdSe/MgSe QWs system is 1.65 μm if uncoupled multiple QWs are used. This emission wavelength would be obtained from a QW thickness of 1.5 nm, which is the minimum thickness that can have two confined states in the well. In order to reach the optical communication wavelength of 1.55 μm, a coupled QW scheme may be used. Fig. 5 shows an example of such a coupled QW structure. It consists of two ZnCdSe wells of 8 and 6 monolayers (MLs) in thickness separated by a 2-ML-thick MgSe barrier. The energy levels and their corresponding wavefunctions were calculated by the envelop function

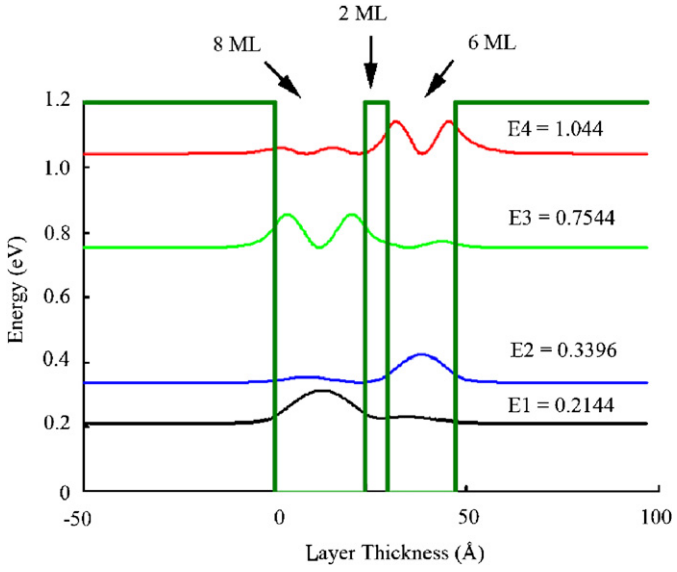

Fig. 5. Calculated electron energy levels and wavefunctions for asymmetric coupled ZnCdSe/MgSe QWs.

approximation. The transition between E1 and E4 yields the wavelength of 1.55 μm. The coupled QW scheme was originally proposed for InGaAs/AlAs QWs [15] and has also been used for the InGaAs/AlAsSb system [16] to achieve short wavelength ISB transition.

4. Summary

In summary, we have shown that, with their large CBO, wide band gap II-selenide semiconductors are promising materials for short wavelength ISB devices. We have observed ISB EL in a ZnCdSe/ZnCdMgSe QC structure at temperatures from 78 to 300 K. ZnCdSe QWs with metastable zincblende MgSe barriers were also grown by MBE. ISB absorption in the 3–5 μm mid-IR region has been observed in the ZnCdSe/MgSe QW structures. Calculations indicate that ISB transitions in the latter material system can reach the optical communication wavelength of 1.55 μm, making it a promising candidate for fabrication of ultrafast all-optical switches.

Acknowledgements

This work is supported in part by MIRTHE (NSF-ERC # EEC-0540832) and PSC-CUNY Research Award (# 61401-0039).

References

[1] F. Cappaso, A.Y. Cho, Surf. Sci. 299–300 (1994) 878.
[2] A.Y. Cho, Molecular Beam Epitaxy, AIP Press, Woodbury, NY, 1994.
[3] J. Faist, F. Capasso, C. Sirtori, D.L. Sivco, A.Y. Cho, in: H.C. Liu, F. Capasso (Eds.), Intersubband Transitions in Quantum Wells: Physics and Device Applications II, Academic, San Diego, 2000, pp. 1–83 (Chapter 1).
[4] H.C. Liu, in: H.C. Liu, F. Capasso (Eds.), Intersubband Transitions in Quantum Wells: Physics and Device Applications I, Academic, San Diego, 2000, pp. 129–196 (Chapter 3).
[5] A. Neogi, in: R. Paiella (Ed.), Intersubband Transitions in Quantum Structures, McGraw-Hill, New York, 2006, pp. 389–425 (Chapter 10).
[6] C. Gmachl, F. Capasso, D.L. Sivco, A.Y. Cho, Rep. Prog. Phys. 64 (2001) 1533.
[7] R. Kohler, R.C. Iotti, A. Tredicucci, F. Rossi, Appl. Phys. Lett. 79 (2001) 3922.
[8] B.S. Williams, H. Callebaut, S. Kumar, Q. Hu, J.L. Reno, Appl. Phys. Lett. 82 (2003) 1015.
[9] Q. Yang, W. Bronner, C. Manz, B. Raynor, H. Menner, Ch. Mann, K. Kohler, J. Wagner, Appl. Phys. Lett. 88 (2006) 201109.

[10] J. Devenson, O. Cathabard, R. Teissier, A.N. Baranov, Appl. Phys. Lett. 91 (2007) 251102.
[11] L. Nevou, M. Tchernycheva, F.H. Julien, F. Guillot, E. Monroy, Appl. Phys. Lett. 90 (2007) 121106.
[12] H. Lu, A. Shen, M.C. Tamargo, C.Y. Song, H.C. Liu, S.K. Zhang, R.R. Alfano, M. Munoz, Appl. Phys. Lett. 89 (2006) 131903.
[13] K.J. Franz, W.O. Charles, A. Shen, A.J. Hoffman, M.C. Tamargo, C. Gmachl, Appl. Phys. Lett. 92 (2008) 121105.
[14] B.S. Li, A. Shen, W.O. Charles, Q. Zhang, M.C. Tamargo, Appl. Phys. Lett. 92 (2008) 261104.
[15] H. Yoshida, T. Mozume, T. Nishimura, O. Wada, Electron. Lett. 34 (1998) 913.
[16] H. Yoshida, T. Mozume, A. Neogi, O. Wada, Electron. Lett. 35 (1999) 1103.